

Mechanism for Orbital Ordering in KCuF_3

E. Pavarini,¹ E. Koch,¹ and A. I. Lichtenstein²

¹*Institut für Festkörperforschung and Institute for Advanced Simulation, Forschungszentrum Jülich, 52425 Jülich, Germany*

²*Institute of Theoretical Physics, University of Hamburg, Jungiusstrasse 9, 20355 Hamburg, Germany*

(Received 18 August 2008; published 31 December 2008)

The Mott insulating perovskite KCuF_3 is considered the archetype of an orbitally ordered system. By using the local-density approximation+dynamical mean-field theory method, we investigate the mechanism for orbital ordering in this material. We show that the purely electronic Kugel-Khomskii superexchange mechanism alone leads to a remarkably large transition temperature of $T_{\text{KK}} \sim 350$ K. However, orbital order is experimentally believed to persist to at least 800 K. Thus, Jahn-Teller distortions are essential for stabilizing orbital order at such high temperatures.

DOI: [10.1103/PhysRevLett.101.266405](https://doi.org/10.1103/PhysRevLett.101.266405)

PACS numbers: 71.10.Fd, 71.10.Hf, 71.27.+a

In a seminal work [1], Kugel and Khomskii showed that in strongly correlated systems with orbital degrees of freedom, many-body effects could give rise to orbital order (OO) via a purely electronic superexchange mechanism. Orbital ordering phenomena are now believed to play a crucial role in determining the electronic and magnetic properties of many transition-metal oxide Mott insulators. While it is clear that Coulomb repulsion is a key ingredient, it remains uncertain whether it just enhances the effects of lattice distortions [2] or really drives orbital order via superexchange [1].

We analyze these two scenarios for the archetype of an orbitally ordered material, KCuF_3 [1]. In this $3d^9$ perovskite, the Cu d -levels are split into completely filled three-fold degenerate t_{2g} -levels and two-fold degenerate e_g -levels, occupied by one hole. In the first scenario, Jahn-Teller elongations of some Cu-F bonds split the partially occupied e_g -levels further into two nondegenerate crystal-field orbitals. The Coulomb repulsion, U , then suppresses quantum orbital fluctuations favoring the occupation of the lower energy state, as it happens in some t_{2g} -perovskites [3,4]. In this picture, the ordering is caused by electron-phonon coupling; Coulomb repulsion just enhances the orbital polarization due to the crystal-field splitting [3,5]. In the second scenario, the purely electronic superexchange mechanism, arising from the e_g -degeneracy, drives orbital ordering, and Jahn-Teller distortions are merely a secondary effect. In this picture, electron-phonon coupling is of minor importance [1].

The key role of Coulomb repulsion is evident from static mean-field LDA + U calculations, which show [6,7] that in KCuF_3 , the distortions of the octahedra are stable with an energy gain $\Delta E \sim 150$ – 200 meV per formula unit, at least an order of magnitude larger than in LDA [6,7] and GGA [7,8]; recent GGA + DMFT [8] calculations yield very similar results, suggesting in addition that dynamical fluctuations play a small role in determining the stable crystal structure of this system. However, these results might merely indicate that the electron-phonon coupling

is underestimated in LDA or GGA, probably due to self-interaction, rather than identifying Kugel-Khomskii superexchange as the driving mechanism for orbital order. This is supported by *ab initio* Hartree-Fock (HF) calculations which give results akin to LDA + U [9]. Moreover, in the superexchange scenario, it remains to be explained why $T_{\text{OO}} \sim 800$ K [10], more than 20 times the 3D antiferromagnetic (AFM) critical temperature, $T_N \sim 38$ K [11,12], a surprising fact if magnetic- and orbital order were driven by the same superexchange mechanism.

In this Letter, we go beyond previous, $T = 0$, LDA + U , and HF works and study the Kugel-Khomskii mechanism using a nonperturbative many-body approach at finite T , the LDA + DMFT method [13], to calculate the transition temperature T_{KK} and identify the origin of orbital order in KCuF_3 . We show that superexchange alone leads to orbital order with $T_{\text{KK}} \sim 350$ K, less than half the experimental value. Thus, Jahn-Teller distortions are essential for driving orbital order above 350 K.

KCuF_3 is a tetragonal perovskite made of Jahn-Teller distorted CuF_6 octahedra enclosed in an almost cubic K cage [14,15]. The Jahn-Teller distortion amounts to a 3.1% elongation or shortening of the CuF distances in the xy -plane. The tetragonal distortion reduces the CuF bond along z by 2.5%, leaving it of intermediate length. The long (l) and short (s) bonds alternate between x and y along all three cubic axes (a -type pattern) [12]. At each site, one hole occupies the highest e_g -orbital, $\sim |s^2 - z^2\rangle$, i.e., the occupied orbitals ($\sim |x^2 - z^2\rangle$ or $\sim |y^2 - z^2\rangle$) alternate in all directions. This ordering and the crystal structure are shown in Fig. 1.

Following the LDA + DMFT scheme presented in Ref. [3], we first calculate the LDA band-structure using the N th-order muffin-tin orbital method (NMTO). We find filled F-bands divided by a gap of ~ 0.8 eV from the d -bands (Fig. 2) of width $W_d \sim 3.2$ eV ($W_{t_{2g}} \sim 1$ eV, $W_{e_g} \sim 2.9$ eV). The energies of the d -crystal-field orbitals (wrt Fermi level) are -2.01 eV, -1.82 eV, and -1.74 eV (t_{2g}) and -1.39 eV and -0.34 eV (e_g). The t_{2g} states are

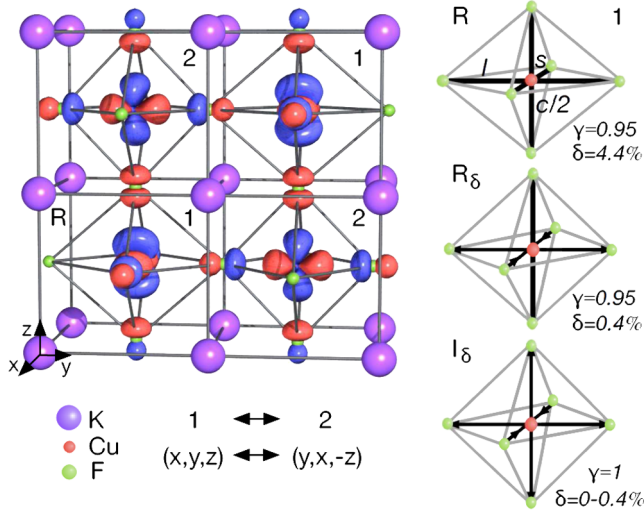


FIG. 1 (color online). Left: Crystal structure and orbital order in a -type [12] KCuF_3 . Cu is at the center of F octahedra enclosed in a K cage. The conventional cell is tetragonal with axes \mathbf{a} , \mathbf{b} , \mathbf{c} , where $a = b$, $c = 0.95a\sqrt{2}$. The pseudocubic axes are defined as $\mathbf{x} = (\mathbf{a} + \mathbf{b})/2$, $\mathbf{y} = (-\mathbf{a} + \mathbf{b})/2$, and $\mathbf{z} = \mathbf{c}/2$. All Cu sites are equivalent. For sites 1, the long (short) bond l (s) is along \mathbf{y} (\mathbf{x}). Vice versa for sites 2. Orbital $|2\rangle$ (see Table I), occupied by one hole, is shown for each site. Right: Jahn-Teller distortions at sites 1, measured by $\delta = (l - s)/(l + s)/2$ and $\gamma = c/a\sqrt{2}$. R is the experimental structure, R_δ and I_δ two ideal structures with reduced distortions, and I_0 is cubic.

completely filled, do not hybridize with the e_g -levels, and thus are likely unimportant for orbital ordering [16]. For the active states, we construct a basis of localized e_g NMTO Wannier functions [3]. The corresponding e_g Hubbard model is

$$H = H^{\text{LDA}} + \sum_{im} U_{m,m} n_{im}^\dagger n_{im} + \frac{1}{2} \sum_{im(\neq m')\sigma\sigma'} (U_{m,m'} - J\delta_{\sigma,\sigma'}) n_{im\sigma}^\dagger n_{im'\sigma'}, \quad (1)$$

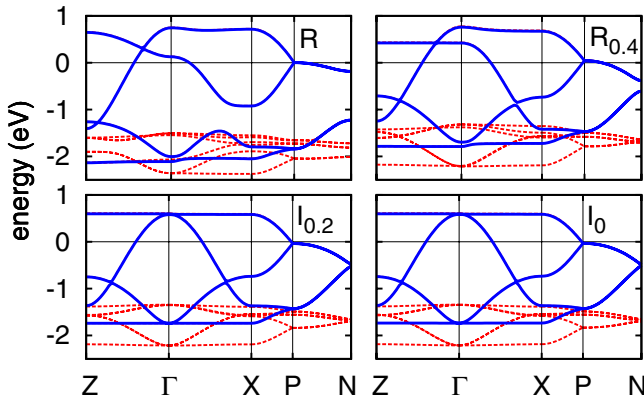


FIG. 2 (color online). LDA 3d-bands (in eV) of KCuF_3 for the real crystal (R) and less distorted structures (see Fig. 1). Lines: e_g -bands. Dashes: t_{2g} -bands. The Fermi level is at zero.

where $n_{im\sigma} = c_{im\sigma}^\dagger c_{im\sigma}$ and $c_{im\sigma}^\dagger$ creates an electron with spin σ in a Wannier orbital $|m\rangle = |x^2 - y^2\rangle$ or $|3z^2 - 1\rangle$ at site i ; the direct and exchange [17] terms of the screened on-site Coulomb interaction are $U_{mm'} = U - 2J(1 - \delta_{m,m'})$ and J . We solve (1) using dynamical mean-field theory in the single-site approximation (DMFT) [18] and its cluster extension (CDMFT) [19], using a quantum Monte Carlo [20] impurity solver and working with the full self-energy matrix $\Sigma_{mm'}$ in orbital space [3]. We obtain the spectral matrix on the real axis by analytic continuation [21]. We use as parameters $J = 0.9$ eV and vary U between 7 and 9 eV. These values are close to the theoretical estimates based on constrained LDA [6].

In the paramagnetic phase, single-site DMFT spectral-function calculations yield a Mott gap of about 2.5 eV for $U = 7$ eV, and 4.5 eV for $U = 9$ eV. The system is orbitally ordered, and the OO is a -type as the distortion pattern; static mean-field (LDA + U , HF) calculations [7,9,22] give similar orbital order, however, also antiferromagnetism. We define the orbital polarization p as the difference in occupation between the most and least occupied natural orbital (diagonalizing the e_g density-matrix). It turns out that to a good approximation, p is given by the difference in occupation between the highest ($|2\rangle$) and the lowest ($|1\rangle$) energy crystal-field orbital, defined in Table I. In Fig. 3, we show p as a function of temperature. We find that the polarization is saturated ($p \sim 1$) even for temperatures as high as 1500 K. We obtain very similar results in two-site CDMFT calculations.

Using second-order perturbation theory, we calculate the exchange-coupling constants for the orbitally ordered state found with DMFT, and obtain [23]

$$J_{SE}^{i,i'} \sim \frac{4|t_{2,2}^{i,i'}|^2(U + \Delta)}{(U + \Delta)^2 - J^2} - \frac{|t_{1,2}^{i,i'}|^2 + |t_{2,1}^{i,i'}|^2}{U + \Delta - 3J} \frac{2J}{U + \Delta - J},$$

where $t_{j,j'}^{i,i'}$ are the hopping integrals from site i to site i' , and $j, j' = 1, 2$ are the e_g crystal-field states. As shown in Table I, the calculated exchange couplings are in very good agreement with experimental findings. Thus, our method gives both the correct orbital order and the correct magnetic structure.

To understand whether this orbital order is driven by the exchange coupling or merely is a consequence of the crystal-field splitting, we consider hypothetical lattices with reduced deformations, measured by $\gamma = c/\sqrt{2}a$ (tetragonal distortion) and $\delta = (l - s)/(l + s)/2$ (Jahn-Teller deformation). To keep the volume of the unit cell at the experimental value, we renormalize all lattice vectors by $(\gamma/0.95)^{-1/3}$. We calculate the Hamiltonian for a number of structures reducing the distortion of the real crystal [13] with $\gamma = 0.95$ and $\delta = 4.4\%$ to the ideal cubic structure $\gamma = 1$ and $\delta = 0$. The bands for some of these structures are shown in Fig. 2. We use the notation R_δ for structures with the real tetragonal distortion $\gamma = 0.95$ and I_δ for ideal

TABLE I. Hopping integrals $t_{j,j'}^{i,i'}$ in the crystal-field basis (j, j') from a site i of type 1 to a neighboring site i' of type 2 in direction $lx + ny + mz$. J_{SE} are the magnetic superexchange couplings for the experimental structure and some representative orbital-superexchange couplings for the ideal cubic structure [23]. The crystal-field states are $|1\rangle = \cos\theta|3l^2 - 1\rangle + \sin\theta|s^2 - z^2\rangle$ and $|2\rangle = -\sin\theta|3l^2 - 1\rangle + \cos\theta|s^2 - z^2\rangle$ where s (l) is the direction of the short (long) bond ($s = x, l = y$ for a site 1). The crystal-field splitting and $\cos\theta$ are given for all structures. All energies are in meV.

Experimental structure R [13]									
lmn	$t_{1,1}^{i,i'}$	$t_{1,2}^{i,i'}$	$t_{2,1}^{i,i'}$	$t_{2,2}^{i,i'}$	$J_{SE}^{i,i'}(\text{th.})$	$J_{SE}^{i,i'}(\text{exp.})$			
001	-83	-161	-161	-343	57	53 [24,25]			
010	98	-352	-17	59	-4	-0.4 [25]			
100	98	-17	-352	59	-4	-0.4 [25]			
Ideal cubic structure I_0									
lmn	$t_{1,1}^{i,i'}$	$t_{1,2}^{i,i'}$	$t_{2,1}^{i,i'}$	$t_{2,2}^{i,i'}$	$J_{SE}^{zz,i,i'}(\text{th.})$	$J_{SE}^{+-i,i'}(\text{th.})$			
001	-93	-163	-163	-282	-162	0			
010	188	-327	-1	0	-40	60			
100	188	-1	-327	0	-40	60			
Crystal-field splittings $\Delta_{2,1}$ and $\cos\theta$									
	R	$R_{0.4}$	R_0	$I_{4,4}$	$I_{0,4}$	$I_{0,2}$	$I_{0,1}$	$I_{0,05}$	I_0
$\Delta_{2,1}$	1050	216	180	845	89	46	22	11	0
$\cos\theta$	0.99	0.950	0.866	0.97	0.97	0.97	0.97	0.97	0.97

($\gamma = 1$) structures. The distortions affect the hopping integrals, both along (001) and in the xy -plane, as shown in Table I. The main effect is, however, the crystal-field splitting $\Delta_{2,1}$ which decreases almost linearly with decreasing distortion, as expected for a Jahn-Teller system. For each structure, we obtain the Hamiltonian H^{LDA} for the e_g -bands and perform LDA + DMFT calculations for decreasing temperatures. At the lowest temperatures, we find a -type OO with full orbital polarization for all structures (see Fig. 3). At 800 K, the situation is qualitatively different. Orbital polarization remains saturated when reducing δ from 4.4% to 1%. For smaller distortions, however, p rapidly goes to zero: For $\delta = 0.2\%$ and $\gamma = 1$, p is already reduced to ~ 0.5 , and becomes negligible in the cubic limit. Thus, superexchange alone is not sufficiently strong to drive orbital ordering at $T \gtrsim 800$ K.

From the temperature dependence of the orbital polarization, we can determine the transition temperature T_{KK} at which the Kugel-Khomskii superexchange mechanism would drive orbital ordering, and thus disentangle the superexchange from the electron-phonon coupling. For this, we study the ideal cubic structure, introducing a negligible (1 meV) crystal-field splitting as an external field to break the symmetry. We find a phase transition to an orbitally ordered state at $T_{\text{KK}} \sim 350$ K. The hole orbi-

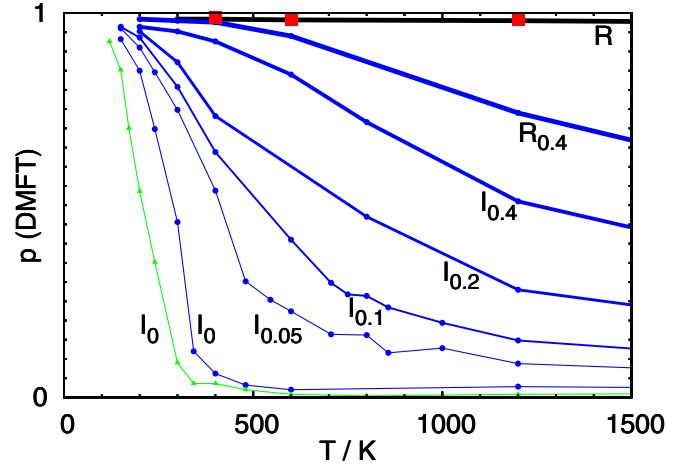


FIG. 3 (color online). Orbital polarization p as a function of temperature calculated with LDA + DMFT (R, circles, triangles). R: $U = 7$ eV, experimental structure. Circles: $U = 7$ eV, idealized structures R_δ and I_δ (see Fig. 1) with decreasing crystal-field. Triangles: $U = 9$ eV, I_0 only. Squares: cluster DMFT for the experimental structure and $U = 7$ eV.

als at two neighboring sites are $\sim |y^2 - z^2\rangle$ and $\sim |x^2 - z^2\rangle$, in agreement with the original prediction of Kugel and Khomskii [1]. This critical temperature is sizable, but significantly smaller than $T_{\text{OO}} \sim 800$ K [10].

Since the screened Coulomb repulsion U is hard to calculate, it is crucial to identify the range of plausible values of U and to estimate how T_{KK} varies in this range. For the experimental structure, $U \sim 5$ eV yields a tiny gap in the DMFT spectral function and $U \sim 6$ eV a semiconducting gap of 1.3 eV, while KCuF_3 is a good insulator [26]. It seems therefore unrealistic that U is smaller than 7 eV. It could, however, be larger. In Fig. 3, we show the results for $U = 9$ eV. We find a reduction to $T_{\text{KK}} \sim 300$ K, reflecting the decrease in the superexchange coupling. Thus, we can conclude that, within single-site DMFT, $T_{\text{KK}} \sim 300\text{--}350$ K, sizable but at least a factor two smaller than $T_{\text{OO}} \sim 800$ K.

The ordering temperature T_{KK} might be even overestimated by the single-site DMFT approximation, as is common for mean-field theories [27]. To investigate the effects of short-range correlations, we therefore perform two-site CDMFT calculations for the cubic structure. We use a supercell containing eight formula units, with axis $\mathbf{a}' = 2\mathbf{x}$, $\mathbf{b}' = 2\mathbf{y}$, $\mathbf{c}' = 2\mathbf{z}$, and a two-site cluster which averages the cubic directions, i.e., imposing $\Sigma^{i,i'} = \Sigma^{i,i\pm x} = \Sigma^{i,i\pm y} = \Sigma^{i,i\pm z}$, for nearest neighbors i and i' in the supercell. For $U = 7$ eV, we find that the polarization starts to increase around 300–350 K, somewhat below the single-site transition.

To compare these results with superexchange theory, we calculate the orbital-superexchange coupling assuming that no long-range magnetic order is present [23]. Two representative couplings are

$$J_{SE}^{zz,ii'} = \sum_{\tau,\tau'} (-1)^{\tau+\tau'} \frac{2|t_{\tau,\tau'}^{ii'}|^2}{U+J} \frac{2U+6J}{U-3J},$$

$$J_{SE}^{+-,ii'} = \sum_{\tau,\tau'} \left[\frac{2t_{\tau,\tau'}^{ii'} t_{\tau',\tau}^{ii'}}{U-J} \frac{2U}{U-3J} + \frac{2t_{\tau,\tau'}^{ii'} t_{\tau',\tau}^{ii'}}{U-J} \frac{2J}{U+J} \right],$$

where we adopt the pseudospin description of the orbital states [1], with $\tau = 1/2$ corresponding to $|3z^2 - 1\rangle$ and $\tau = -1/2$ to $|x^2 - y^2\rangle$. These couplings, shown in Table I, are very anisotropic, with the largest about 3 times the magnetic exchange coupling along \mathbf{z} . Again, this suggests that T_{KK} should be larger than $T_N = 38$ K, but certainly smaller than $T_{OO} \sim 800$ K.

All this indicates that in KCuF_3 , the driving mechanism for orbital ordering is not pure superexchange. Further support comes from an accurate reanalysis of LDA + U results. To do this, we first perform LDA + U calculations for the cubic and distorted structure [7], and obtain results in agreement with previous literature [6,22]. For the undistorted KCuF_3 , we find a fully orbitally polarized solution, and the occupation matrix only slightly differs from that obtained for the experimental structure. This shows that the energy gain due to the distortions, $\Delta E \sim 180$ meV per formula unit, cannot be ascribed to the orbital polarization itself, but rather is an estimate of the electron-phonon coupling, enhanced by self-interaction correction [7]. In order to estimate the energy gain due to orbital polarization, we performed several LDA + U calculations for the cubic structure with different (fixed) occupation matrices. We find that the energy gain [1] is ~ 90 meV, only half of ΔE .

In conclusion, we have calculated the Kugel-Khomskii transition temperature for KCuF_3 and find a remarkably large $T_{KK} \sim 350$ K. Nevertheless, the superexchange mechanism is not sufficiently strong to explain $T_{OO} \sim 800$ K: at such a transition both superexchange and electron phonon coupling are of comparable importance. The assignment $T_{OO} \sim 800$ K [10] is however based on the temperature dependence of the orbital peak intensity signals measured by resonant x-ray scattering [10]. A direct measurement of the evolution of the distortions with temperature would be highly desirable. Should orbital order persist till melting, the electron-phonon coupling contribution would be the dominant mechanism.

We acknowledge discussions with and helpful comments from D. I. Khomskii and P. Ghigna. The calculations were performed on the Jülich BlueGene under account JIFF2200.

- [1] K. I. Kugel and D. I. Khomskii, Zh. Eksp. Teor. Fiz. **64**, 1429 (1973) [Sov. Phys. JETP **37**, 725 (1973)]. To estimate from LDA + U the energy gain due to orbital polarization, we fitted Eq. 9.
- [2] B. Halperin and R. Engelman, Phys. Rev. B **3**, 1698 (1971).

- [3] E. Pavarini *et al.*, Phys. Rev. Lett. **92**, 176403 (2004); E. Pavarini, A. Yamasaki, J. Nuss, and O. K. Andersen, New J. Phys. **7**, 188 (2005).
- [4] M. De Raychaudhury, E. Pavarini, and O. K. Andersen, Phys. Rev. Lett. **99**, 126402 (2007).
- [5] See also A. I. Poteryaev *et al.*, Phys. Rev. B **78**, 045115 (2008).
- [6] A. I. Liechtenstein, V. I. Anisimov, and J. Zaanen, Phys. Rev. B **52**, R5467 (1995).
- [7] E. Koch and E. Pavarini (to be published); we used PAW as implemented in ABINIT (www.abinit.org) and the LAPW exciting code (exciting.sourceforge.net).
- [8] I. Leonov *et al.*, Phys. Rev. Lett. **101**, 096405 (2008).
- [9] M. D. Towler, R. Dovesi, and V. R. Saunders, Phys. Rev. B **52**, 10150 (1995).
- [10] L. Paolasini *et al.*, Phys. Rev. Lett. **88**, 106403 (2002).
- [11] M. T. Hutchings, E. J. Samuelsen, G. Shirane, and K. Hirakawa, Phys. Rev. **188**, 919 (1969).
- [12] There are two stable polytypes [13]. In the a -type, the l bonds alternate between x and y along all three cubic axes, while in the d -type, only along x and y ; the magnetic structure is A -type AFM for both polytypes, and $T_N = 22$ K for the d -type [11]. Here for simplicity, we focus on the a -type, the most commonly found.
- [13] V. I. Anisimov *et al.*, J. Phys. Condens. Matter **9**, 7359 (1997); A. I. Liechtenstein and M. I. Katsnelson, Phys. Rev. B **57**, 6884 (1998).
- [14] A. Okazaki, J. Phys. Soc. Jpn. **26**, 870 (1969).
- [15] A tiny displacement of the apical F away from the Cu-Cu bond was reported in M. Hidaka, T. Eguchi, and I. Yamada, J. Phys. Soc. Jpn. **67**, 2488 (1998). We neglect this distortion in the present study.
- [16] For the experimental structure, we performed LDA + DMFT calculations for the $5d$ -band Hubbard model. We find that the t_{2g} -bands are just shifted to lower energy and broadened. The e_g spectral-function shows a gap of ~ 2.5 eV and is almost identical to that obtained solving the 2-band e_g Hubbard model (with t_{2g} downfolded) for the same parameters.
- [17] J. Kanamori, Prog. Theor. Phys. **30**, 275 (1963).
- [18] A. Georges, G. Kotliar, W. Kraut, and M. J. Rozenberg, Rev. Mod. Phys. **68**, 13 (1996).
- [19] Th. Maier, M. Jarrell, Th. Pruschke, and M. Hettler, Rev. Mod. Phys. **77**, 1027 (2005).
- [20] J. E. Hirsch and R. M. Fye, Phys. Rev. Lett. **56**, 2521 (1986).
- [21] J. E. Gubernatis, M. Jarrell, R. N. Silver, and D. S. Sivia, Phys. Rev. B **44**, 6011 (1991).
- [22] N. Binggeli and M. Altarelli, Phys. Rev. B **70**, 085117 (2004).
- [23] We adopt the following conventions for the superexchange couplings. Spin-spin interaction: $\frac{1}{2} \sum_{i,j} J_{SE}^{ij} S_i \cdot S_j$, where i and j are the lattice sites. Orbital-orbital interaction: $\frac{1}{2} \sum_{i,i',\mu,\mu'} J_{SE}^{\mu\mu'ii'} T_i^\mu \cdot T_{i'}^{\mu'}$, where $\mu, \mu' = x, y, z$, and T are pseudospin $1/2$ operators [1].
- [24] D. A. Tennant *et al.*, Phys. Rev. B **52**, 13381 (1995).
- [25] S. K. Satija *et al.*, Phys. Rev. B **21**, 2001 (1980).
- [26] P. Ghigna (private communication).
- [27] H. E. Stanley, *Introduction to Phase Transitions and Critical Phenomena* (Oxford University Press, New York, 1971).